J. Wind Eng. Ind. Aerodyn. 98 (2010) 533–547

Contents lists available at ScienceDirect

Journal of Wind Engineering and Industrial Aerodynamics

journal homepage: www.elsevier.com/locate/jweia

Surface wind measurements in three Gulf Coast hurricanes of 2005

Forrest J. Masters [a,*], Henry W. Tieleman [b], Juan A. Balderrama [a]

[a] Civil and Coastal Engineering, 365 Weil Hall, University of Florida, Gainesville, FL 32611, USA
[b] Engineering Science and Mechanics, Virginia Polytechnic Institute and State University, 330 Norris Hall, Blacksburg, VA 24061, USA

ARTICLE INFO

Article history:
Received 3 June 2008
Received in revised form
20 April 2010
Accepted 23 April 2010
Available online 11 June 2010

Keywords:
Tropical cyclone (hurricane)
Turbulence
Integral length scale
Gust factor

ABSTRACT

Detailed observations from surface layer experiments in the path of Atlantic hurricanes are presented in this paper. The purpose is to obtain information that will aid in the reduction of hurricane wind damage to residential structures by providing input for wind tunnel and full-scale flow simulation experiments that assess wind loads on these structures under hurricane conditions. The contents of the paper document the mean flow and turbulence characteristics from data recorded by nine mobile instrumented towers deployed at coastal locations near the anticipated path of each of the three hurricanes (Katrina, Rita, and Wilma) that made landfall on the US coast along the Gulf of Mexico in 2005. Wind data were collected at two elevations (5 and 10 m) from these towers by the Florida Coastal Monitoring Program, a joint research program led by the University of Florida and the Institute for Business and Home Safety.

Published by Elsevier Ltd.

1. Introduction

While numerous field experiments have been conducted in the last century to characterize wind in neutral conditions (e.g., Izumi, 1971), the literature is scarce in addressing surface-level winds occurring over land in tropical cyclones. This information is critical for many active areas in wind engineering research, including active gust generation in wind tunnels (e.g., Haan et al., 2006) and full-scale test facilities to evaluate building components (e.g., Salzano et al., 2010). Recent analyses are largely restricted to open exposure measurements collected in a single hurricane (e.g., Schroeder and Smith, 2003) or a few hurricanes (e.g., Yu et al., 2008). The purpose of this paper is to add to this knowledge base through the analysis of data collected from portable instrumented towers deployed by the Florida Coastal Monitoring Program (FCMP, fcmp.ce.ufl.edu) during three notable hurricanes in 2005: Katrina, Rita, and Wilma (Table 1). The FCMP is a research consortium – led by the University of Florida and the Institute for Business and Home Safety – that focuses on full-scale experimental methods to quantify near-surface hurricane wind behavior and their resultant loads on residential structures. Since 1998, the FCMP has collected over 50 observations in more than 20 named storms in Alabama, Florida, Louisiana, Mississippi, North Carolina, and Texas.

2. Instrumentation

The FCMP towers (shown in Fig. 1) are designed to resist a 90 m/s peak gust wind speed—this corresponds to a Category 5 hurricane on the Saffir-Simpson Hurricane Wind Scale (www.nhc.noaa.gov/aboutsshws.shtml). Three levels of sensors outfit the tower at elevations of 3, 5, and 10 m. The data acquisition system measures 3D wind speed and direction at the two upper levels and collects temperature, rainfall, barometric pressure, and relative humidity data at the tower's base. Two RM Young anemometer systems – a wind monitor (Model no. 05103 V) and a custom array of three gill propellers (Model no. 27106 R) – collect data at the 10 m level. A second array of gill propellers collects wind speed data at the 5 m level to measure winds at the approximate mean roof height of a single-story home. Dynamic characteristics of the anemometer's four-blade polypropylene helicoid propellers (Model no. 08234) include a 2.7 m 63% recovery distance constant and a damped natural wavelength of 7.4 m. The wind monitor is rated for a 100 m/s gust survival and has a 50% recovery vane delay distance of 1.3 m. The limitations caused by its frequency response characteristics are detailed in Schroeder and Smith (2003). The wind monitor serves as a redundant system by providing a second set of 10 m wind velocity data that is used to quality control the data recorded by the primary system (the array of three gill propellers).

The system described is capable of making velocity observations on a continuous basis with a sampling frequency of 10 Hz. Data observations are recorded, post-processed, uploaded in real-time, and made available from the FMCP web site (http://fcmp.ce.ufl.edu) within minutes, providing mean wind and turbulence characteristics of the surface flow without interruptions for at least 24 h.

* Corresponding author. Tel.: +3 5 2 392 9537x1505; fax: 3 5 2 392 3394.
E-mail addresses: masters@ce.ufl.edu (F.J. Masters), tieleman@vt.edu (H.W. Tieleman), jbalderr@ufl.edu (J.A. Balderrama).

0167-6105/$ - see front matter Published by Elsevier Ltd.
doi:10.1016/j.jweia.2010.04.003

Table 1
Hurricanes of 2005: Mobile towers and periods of data acquisition (UTC).

Hurricane	Tower	# of files	Data acquisition		Passage of eye or velocity peak	
			Begin	End	Begin	End
Katrina	T0	92	28-Aug-05 15:04	29-Aug-05 13:49	29-Aug-05 12:00	29-Aug-05 14:00
	T1	104	28-Aug-05 21:43	29-Aug-05 23:28	29-Aug-05 11:00	29-Aug-05 12:00
	T2	56	29-Aug-05 02:37	29-Aug-05 16:22	29-Aug-05 11:00	29-Aug-05 12:00
Rita	T0	92	23-Sep-05 16:54	24-Sep-05 15:39	24-Sep-05 08:00	24-Sep-05 09:00
	T3	74	24-Sep-05 02:00	24-Sep-05 20:15	24-Sep-05 08:00	24-Sep-05 11:00
	T5	102	23-Sep-05 21:00	24-Sep-05 22:15	24-Sep-05 08:00	24-Sep-05 10:00
Wilma	T0	75	23-Oct-05 22:55	24-Oct-05 17:25	24-Oct-05 10:00	24-Oct-05 12:00
	T1	57	24-Oct-05 07:54	24-Oct-05 21:54	24-Oct-05 11:30	24-Oct-05 14:30
	T2	62	24-Oct-05 01:19	24-Oct-05 16:34	24-Oct-05 11:00	24-Oct-05 13:00

Fig. 1. Florida Coastal Monitoring Program tower platform shown in the foreground. Stowed tower shown in the background.

3. Data analysis

The gill anemometers are mounted on the tower such that the bisector of the solid angle formed by the three anemometers is horizontal. Consequently, the obtained data must be transformed from the anemometer-oriented coordinate system to the mean wind coordinate system with the u and v components in the horizontal plane and the w component vertically upward. The x-coordinate is oriented towards the direction of the mean flow, the y-coordinate is perpendicular to the x-direction in the horizontal plane, and the z-coordinate is directed vertically upward to form a right-handed coordinate system. This transformation must be performed for each of the simultaneous observations recorded by the system of anemometers at each level and repeated at each time step to obtain a continuous time history for each sample record.

The discussion in this paper is based on results obtained for the 15-min time histories of each sample record, including the mean velocity U and its direction, and the three turbulence intensity components σ_a/U for $a=u$, v, and w, respectively. Also obtained were the three covariances uw, uv, and vw, the turbulence integral scales for the three velocity components, and the maximum 3 s gust for each sample record.

4. Tower locations

Only observations from those towers that were the closest to the path of the respective hurricanes were considered for analysis in this paper. Tower locations are shown in Fig. 2 and their GPS coordinates are provided in Table 2. The perpendicular distance from the tower location to the path of the hurricane ranged from 3.2 km (Rita, tower T3) to 74 km (Katrina, tower T2) with a mean distance of 28.8 km for all nine deployments. For a tower located directly in the path of the hurricane eye, one can expect air velocity to increase, then stall during a calm period, and subsequently, increase abruptly as the eye passes the tower location. For a tower located outside the eye at all times, the velocity exhibits just a single peak. Katrina T1, and Rita T0 experienced single peaks. The remaining towers employed for this research were subjected to the passage of a hurricane eye; thus, they sustained a double velocity peak.

In general, the towers were deployed in open terrain, mostly areas with uniform roughness within a radial distance of 400 m from the tower location. The exceptions are towers T3 and T5 in Hurricane Rita; the former was located downwind of a subdivision when the winds traveled from the north, while the latter was situated 100 m from tall trees when the winds traveled from the north and west. The average distance from the coast, measured parallel to the path of the hurricane, for the nine towers (three for each hurricane) was 41.8 km.

5. Mean wind speeds

The passage of the eye of a hurricane through a tower location is characterized by increasing wind speeds followed by a relatively short period of calm winds, after which the wind velocity increases again to a second maximum before gradually decreasing as the hurricane moves away from the tower. This variation of the mean wind distribution over time is depicted in Figs. 3 and 4 for Wilma tower T0 and Rita tower T5, respectively. Some of the observed wind distributions, Katrina towers T0 and T1 (Fig. 5) and Rita tower T0, do not exhibit this typical wind pattern, instead they show a single maximum. The observations of the Katrina T0 tower were abruptly terminated due to a power failure and did not record the maximum speed. The wind direction change of 180° during the passage of the eye or after the single peak wind speeds was observed in all other cases. For towers located on the starboard side of the hurricane path, the mean wind rotates in a clockwise fashion; while for those located on its port side, the mean wind rotates in the opposite direction as the eye or the peak passes (Table 3).

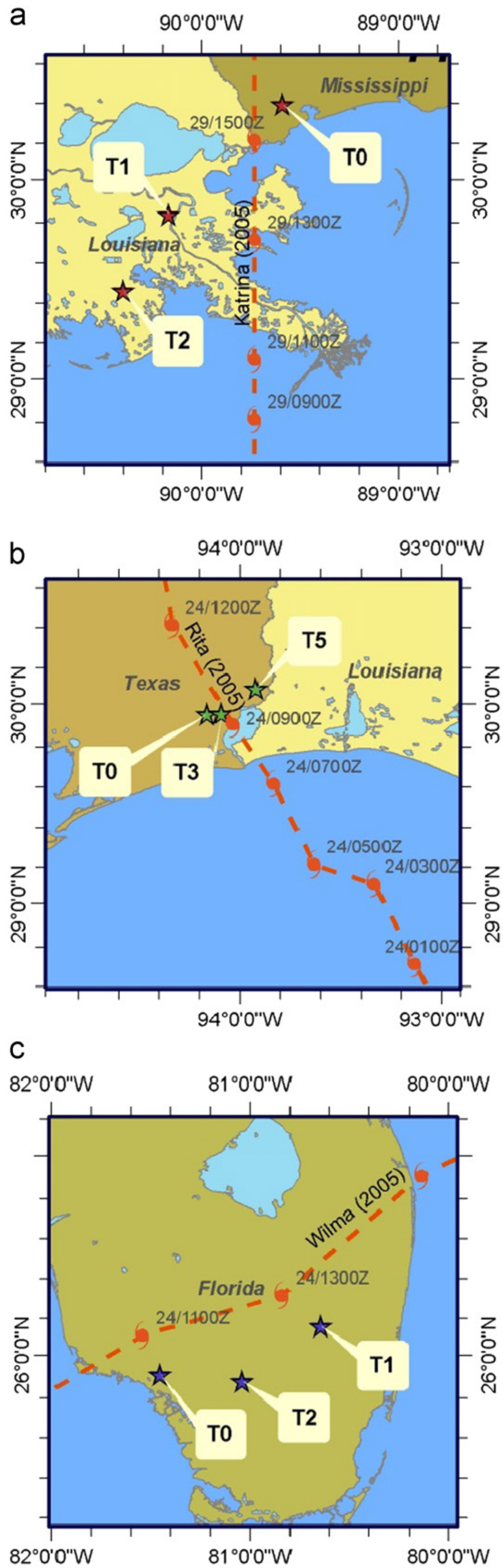

Fig. 2. Location of FCMP towers during Hurricanes: (a) Katrina, (b) Rita, and (c) Wilma.

The maximum observed 15-min wind speeds at the 10 m level varied between 23.0 and 36.0 m/s, while the maximum 60 s wind speeds varied between 29.2 and 41.9 m/s. The latter indicates that adjusting for terrain, the intensity of the hurricanes at the tower locations fell in the category 1 or below according to the Saffir-Simpson Hurricane Wind Scale (www.nhc.noaa.gov/aboutsshws.shtml).

Table 2
GPS coordinates of the mobile towers.

Hurricane	Tower	Latitude	Longitude
Katrina	T0	30.3801	−89.4551
	T1	29.8253	−90.0319
	T2	29.4441	−90.2628
Rita	T0	29.9512	−94.0220
	T3	29.9548	−93.9542
	T5	30.0797	−93.7841
Wilma	T0	25.9008	−81.3114
	T1	26.1458	−80.5067
	T2	25.8681	−80.8997

6. Turbulence intensities

Near surface turbulence is caused by the earth's landscape, which acts as a momentum sink (Wieringa, 1993). It has been suggested that organized storm features aloft can contribute to or possibly modulate surface level wind characteristics owing to their convective nature (Bradbury et al., 1994; Wurman and Winslow, 1998). Based on 15-min turbulence intensities for each of the towers that experienced an eyewall passage, it appears that the turbulence intensities were not affected by the passage of the hurricane eye. Instead, the turbulence intensities depend primarily on the roughness of the upwind terrain.

The records were partitioned into two sections for which the wind direction range was approximately 30°; Katrina T0 was the exception, producing only one section. Average values for turbulence intensities at 5 and 10 m for each partition, along with their corresponding wind direction ranges, are shown in Table 4. Partitions (a) and (b) for Katrina T1 (Fig. 6), Katrina T2, Rita T0, and Wilma T1 and partition (b) for Rita T3 and T5 (Group 1) exhibit average turbulence intensities at 10 m, $\sigma_u/U=16.8\%$, $\sigma_v/U=12.4\%$, and $\sigma_w/U=6.8\%$, corresponding to relatively smooth terrain; these results are similar to the 5 min turbulence intensities ($\sigma_u/U=17.6\%$, $\sigma_v/U=16.4\%$, and $\sigma_w/U=8.5\%$) obtained by Schroeder and Smith (2003) for an airport exposure during Hurricane Bonnie of 1998. On the other hand, partitions (a) and (b) for Wilma T0 and T2, partition (a) for Rita T3 and T5 (Fig. 7), and the partition for Katrina T0 (Group 2) produced higher values for the averaged turbulence intensities at 10 m, $\sigma_a/U=23.2\%$, 17.8%, and 10.4% for $a=u$, v, and w respectively; Schroeder et al. (2009) performed a similar analysis from 10.7 m data for seven tropical cyclones and obtained a comparable average longitudinal turbulence intensity value, 23.8%, for rough terrain (9.00 cm $< z_0 <$ 18.99 cm). The lower values of σ_u/U and σ_v/U obtained for the first group of partitions are associated with terrain whose aerodynamic roughness length, z_0, is of the order of 1–3 cm. The higher turbulence intensities observations (Group 2) have corresponding z_0 values of 13.3 and 7.2 cm for σ_u/U and σ_v/U, respectively.

Observed averages of σ_u/σ_v and σ_u/σ_w are 1.34 and 2.38, respectively. The limited frequency response of the propeller anemometers may lead to partial filtering of the higher frequencies of the vertical velocity component, thus resulting in values systematically larger than the customary value of 2.0 for σ_u/σ_w. Plots of u and w spectra reveal that the vertical-velocity spectrum is shifted towards higher frequencies with respect to the u-spectrum.

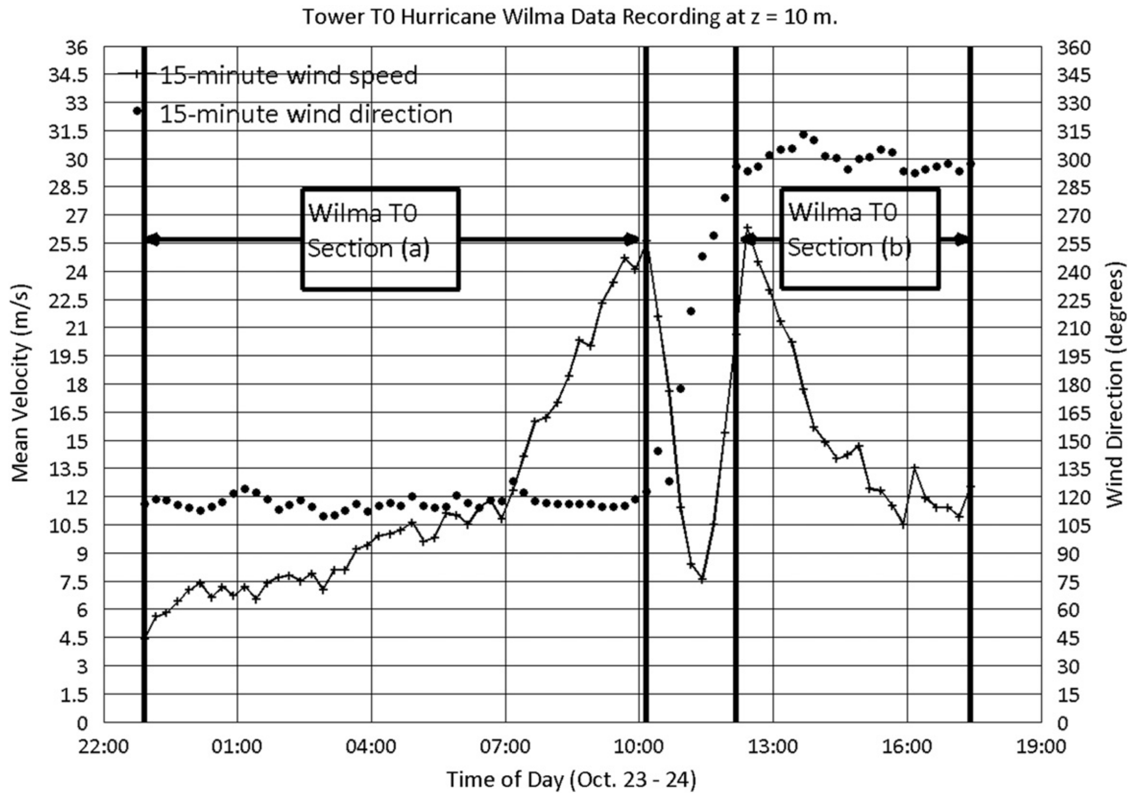

Fig. 3. Mean wind and direction observations from tower T0, Hurricane Wilma (UTC).

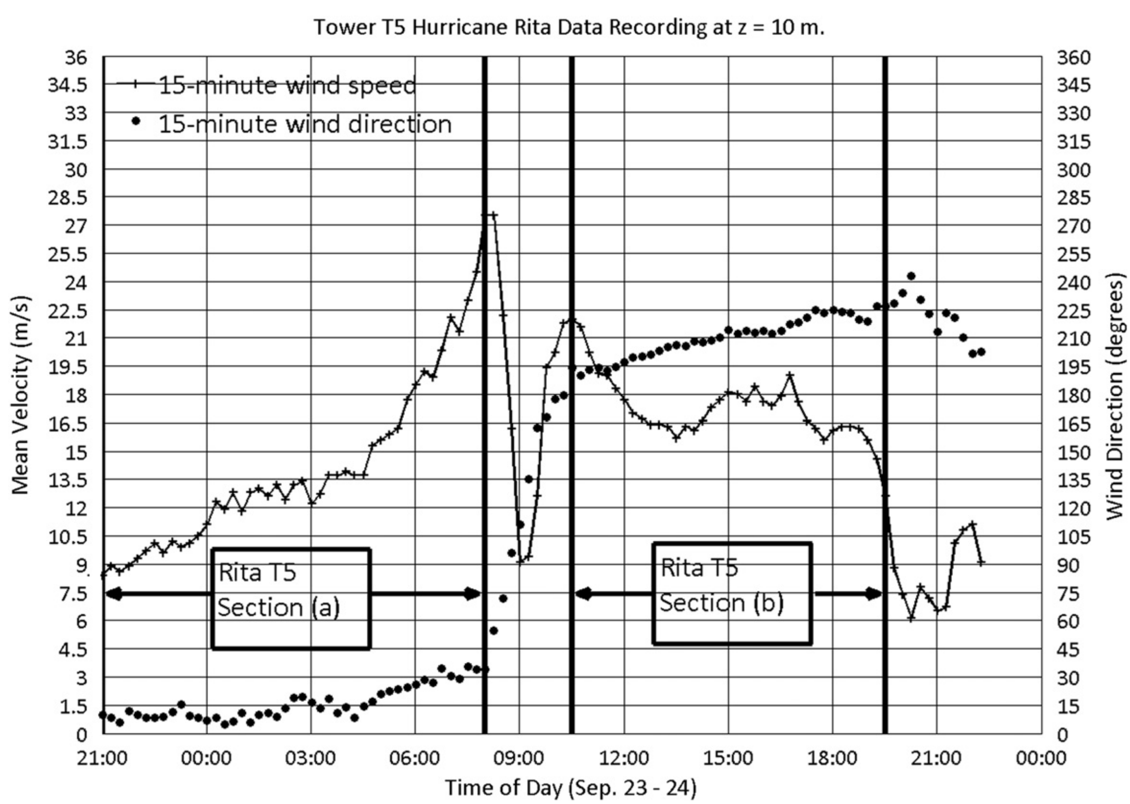

Fig. 4. Mean wind and direction observations from tower T5, Hurricane Rita (UTC).

Consequently, the limited frequency response of the anemometers will affect σ_w more than σ_u, and the ratio σ_u/σ_w is expected to be larger than normal value of 1.92 (Panofsky and Dutton, 1984).

Some of the turbulence intensities, especially those from the Rita towers, reveal a decrease in magnitude with increasing mean velocity before the eye passes the tower location. For example, the

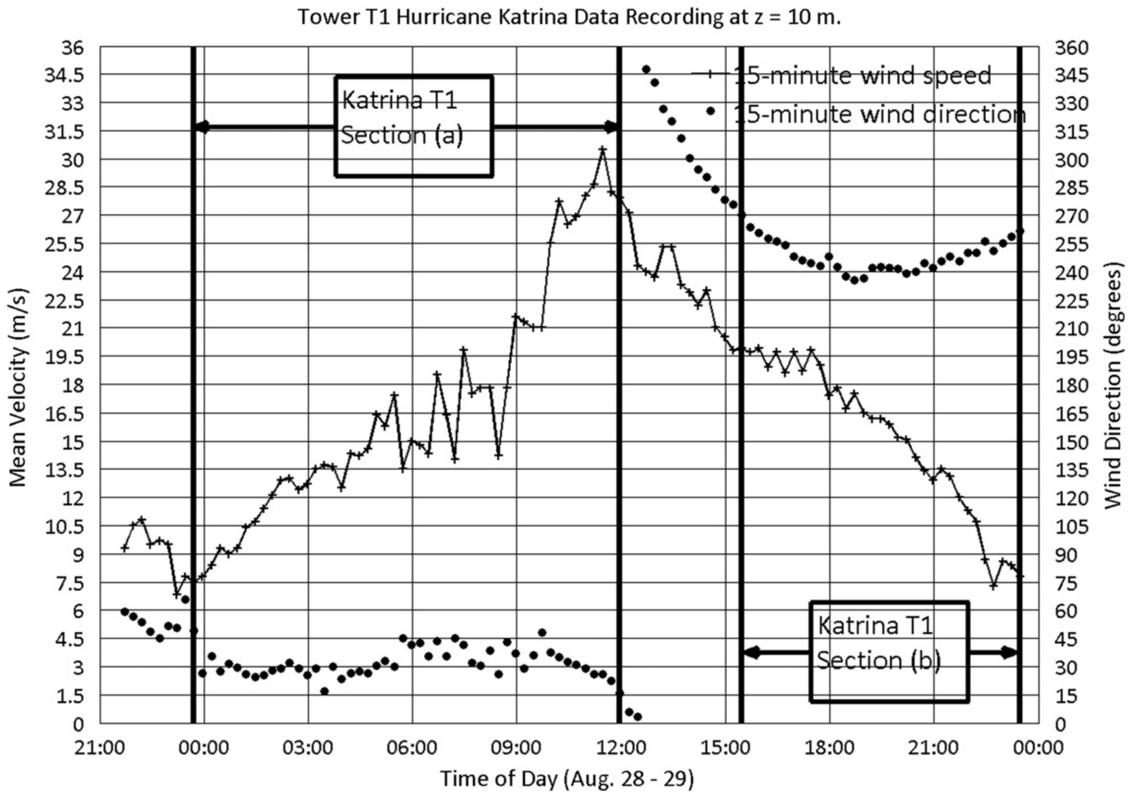

Fig. 5. Mean wind and direction observations from tower T1, Hurricane Katrina (UTC).

Table 3
Maximum velocities and wind direction rotation.

Hurricane and tower	Height, m	Velocity peaks	Change in wind direction, degrees	Maximum mean velocity (m/s)		Maximum 3-s gust (m/s)	
				First peak	Second peak	First peak	Second peak
Katrina T0	5	–	+60	24.1	–	37.9	–
	10	–	+60	26.0	–	40.6	–
Katrina T1	5	Single	−175	25.3	–	40.5	–
	10	Single	−160	30.5	–	45.2	–
Katrina T2	5	Double	−130	25.6	25.0	40.3	36.6
	10	Double	−130	28.3	28.9	42.3	41.9
Rita T0	5	Single	−150	33.0	–	47.4	–
	10	Single	−150	36.0	–	50.0	–
Rita T3	5	Double	−140	20.7	14.7	35.7	24.5
	10	Double	−150	23.8	18.3	39.8	27.8
Rita T5	5	Double	+200	27.2	20.9	42.4	28.1
	10	Double	+200	27.5	22.0	42.4	29.0
Wilma T0	5	Double	+185	23.0	23.1	37.4	39.0
	10	Double	+185	25.6	26.3	38.0	42.5
Wilma T1	5	Double	+160	25.4	28.0	42.4	39.2
	10	Double	+150	34.3	35.3	45.6	44.9
Wilma T2	5	Double	+160	27.8	22.3	40.1	41.9
	10	Double	+160	29.7	27.0	41.6	48.4

Note: Katrina T0 tower experienced a power failure and did not record the maximum wind speed.

10 m longitudinal turbulence intensity at tower T5 decreased approximately (25–20%)/25% = 20% near the approach of the eyewall (Fig. 7). This trend occurred because of experimental design and is not related to the storm's passage. The towers were intentionally oriented so that the maximum winds occurred in the direction corresponding to the least built-up terrain.

7. Friction velocity, U^*

Covariances of the fluctuating velocity components were obtained from the time histories of the u, v, and w components of each 15 min sample record. It was found that the uw covariance has mostly negative values, as expected in a standard boundary

Table 4
Turbulence intensities with standard deviations (%).

Hurricane and tower	$\sigma_u/U \pm$ StD	$\sigma_v/U \pm$ StD	$\sigma_w/U \pm$ StD	Mean wind direction (deg)	Wind direction range (deg)	Segment range
Observations at z=5 m						
Katrina T0	25.72 ± 4.14	22.84 ± 2.05	8.29 ± 1.24	63	43–80	75–92
Katrina T1 (a)	17.35 ± 3.52	14.22 ± 5.51	11.82 ± 1.47	33	16–47	9–58
Katrina T1 (b)	24.29 ± 4.47	16.09 ± 2.69	9.14 ± 0.99	244	226–276	70–104
Katrina T2 (a)	18.29 ± 1.79	14.97 ± 2.16	6.47 ± 0.52	24	5–38	1–31
Katrina T2 (b)	17.69 ± 1.03	12.85 ± 0.87	6.15 ± 1.12	273	261–295	46–56
Rita T0 (a)	17.82 ± 1.44	13.85 ± 2.01	4.94 ± 0.62	6	−11–21	1–61
Rita T0 (b)	16.02 ± 0.98	12.40 ± 0.88	5.87 ± 0.67	230	220–247	72–92
Rita T3 (a)	32.46 ± 2.15	24.21 ± 2.85	15.57 ± 1.90	358	341–366	1–27
Rita T3 (b)	21.27 ± 1.63	12.94 ± 1.15	10.67 ± 1.55	224	218–237	33–71
Rita T5 (a)	24.88 ± 2.51	20.43 ± 1.87	8.52 ± 1.08	16	7–33	1–45
Rita T5 (b)	17.06 ± 1.68	11.49 ± 0.78	5.40 ± 0.30	211	192–227	55–91
Wilma T0 (a)	22.96 ± 5.06	16.47 ± 1.58	8.68 ± 2.41	117	109–129	1–46
Wilma T0 (b)	23.83 ± 2.98	16.59 ± 1.09	10.00 ± 0.61	301	295–314	54–75
Wilma T1 (a)	23.68 ± 3.26	13.16 ± 2.50	7.64 ± 1.43	126	117–139	1–17
Wilma T1 (b)	17.11 ± 1.30	10.39 ± 2.70	7.44 ± 1.12	277	258–294	25–57
Wilma T2 (a)	23.55 ± 2.24	16.39 ± 2.35	11.07 ± 2.09	136	121–165	1–40
Wilma T2 (b)	22.08 ± 2.06	16.08 ± 1.60	12.93 ± 1.72	287	269–296	47–62
Observations at z=10 m						
Katrina T0	24.88 ± 3.75	21.14 ± 2.00	10.39 ± 0.56	67	47–83	75–92
Katrina T1 (a)	17.14 ± 2.69	14.37 ± 4.15	7.08 ± 0.29	32	16–49	9–58
Katrina T1 (b)	16.73 ± 1.72	12.87 ± 1.27	7.00 ± 0.44	248	235–270	72–104
Katrina T2 (a)	16.84 ± 1.87	12.53 ± 2.19	7.99 ± 0.51	23	8–37	1–31
Katrina T2 (b)	15.91 ± 1.50	11.97 ± 0.76	6.70 ± 0.84	272	260–294	46–56
Rita T0 (a)	16.98 ± 1.23	13.02 ± 2.05	5.74 ± 0.70	7	−10–23	1–61
Rita T0 (b)	15.45 ± 0.92	12.36 ± 0.60	6.05 ± 0.41	231	221–249	72–92
Rita T3 (a)	29.06 ± 1.85	19.06 ± 1.40	12.18 ± 1.37	3	−15–10	1–27
Rita T3 (b)	18.69 ± 1.88	12.68 ± 1.47	8.71 ± 1.17	226	219–245	33–71
Rita T5 (a)	24.35 ± 2.38	21.22 ± 1.80	10.80 ± 1.51	16	5–36	1–45
Rita T5 (b)	16.70 ± 1.50	11.79 ± 0.62	6.48 ± 0.30	210	190–227	55–91
Wilma T0 (a)	20.16 ± 4.65	13.86 ± 1.70	9.32 ± 3.51	117	110–128	1–46
Wilma T0 (b)	20.75 ± 3.28	17.24 ± 1.21	10.34 ± 0.83	299	293–313	54–75
Wilma T1 (a)	18.13 ± 1.91	11.22 ± 1.30	6.46 ± 0.93	132	125-–143	1–17
Wilma T1 (b)	15.72 ± 1.74	11.41 ± 2.32	6.21 ± 0.78	284	270–295	25–57
Wilma T2 (a)	21.50 ± 2.31	16.27 ± 1.96	9.63 ± 2.07	133	120–161	1–40
Wilma T2 (b)	21.41 ± 1.70	15.93 ± 1.79	9.93 ± 1.10	285	269–296	47–62

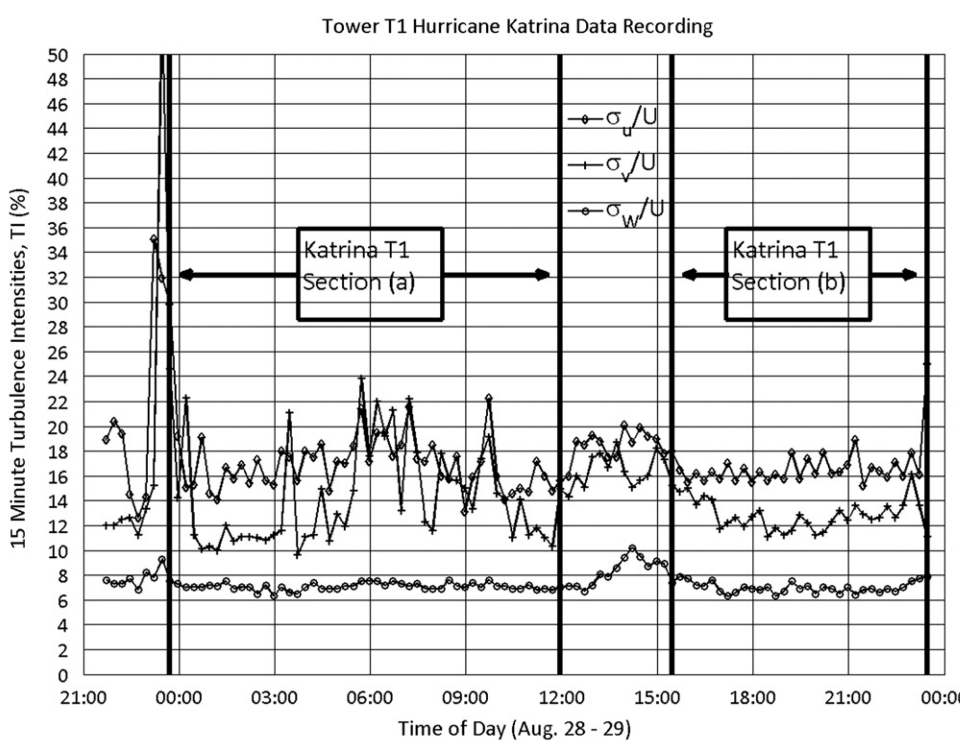

Fig. 6. 15 min, 10 m turbulence intensity observations from tower T1 during Hurricane Katrina (passage of the eye between 11:00 and 12:00 UTC).

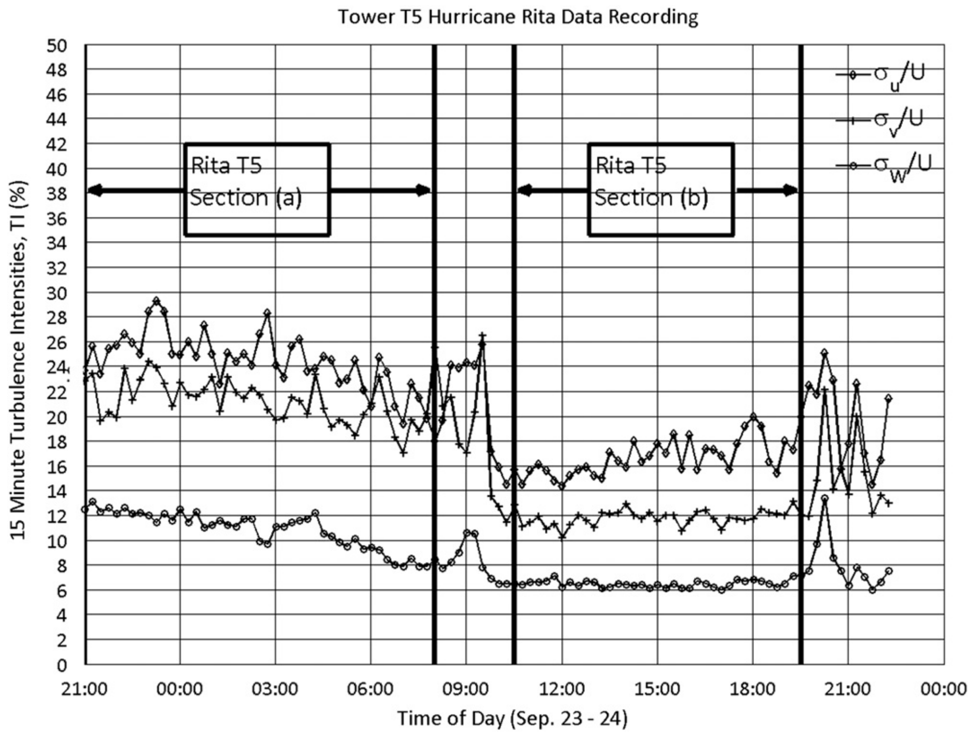

Fig. 7. 15 min, 10 m turbulence intensity observations from tower T5 during Hurricane Rita (passage of the eye between 08:00 and 10:00 UTC).

Table 5
Distribution of positive and negative uw covariances.

Hurricane and tower	# of files	Height (m)	# of files with *uw* covariances	
			Negative values	Positive values
Katrina T0	92	5	22	70
		10	90	2
Katrina T1	104	5	45	59
		10	104	0
Katrina T2	56	5	53	3
		10	49	7
Rita T0	92	5	80	12
		10	92	0
Rita T3	74	5	74	0
		10	74	0
Rita T5	102	5	40	62
		10	0	102
Wilma T0	75	5	75	0
		10	54	21
Wilma T1	57	5	57	0
		10	51	6
Wilma T2	62	5	59	3
		10	58	4

layer under thermally neutral conditions (Table 5). The presence of positive values indicates that the turbulent momentum flux is away from the boundary rather than towards it.

For the Rita T5 tower, which had tall trees to the north and west at a distance of about 100 m, the *uw* covariance at the 10-m level was entirely positive and 61% of its 5-m level values were positive. For the remaining eight towers, the mean percentage of negative averaged *uw* covariance was 80% at the 10 m level and 65% at the 5 m level. The friction velocity for each sample record was obtained from the quartic root of the resultant of the two horizontal turbulent stresses, *uw* and *vw* (Weber, 1999). These results were then used to obtain the turbulence ratios, σ_a/U^*, and to estimate values for the roughness length, z_0.

The averaged turbulence ratios from the hurricane observations are $\sigma_a/U^*=3.09$, 2.36, and 1.29 for $a=u$, v, and w, respectively (Table 6). These results compare reasonably well with the flat, uniform, and smooth multi-terrain observations reported by Högström (1990), for which $\sigma_a/U^*=2.78$, 2.44, and 1.24 for $a=u$, v, and w, respectively.

8. Aerodynamic roughness length, z_0

Since roughness lengths based on mean velocities at two levels must not be used, one must resort to turbulence observations to obtain more reliable values for the roughness lengths. These lengths are evaluated using the hurricane data and Eqs. (1)

Table 6
Nondimensional turbulence ratios.

Hurricane and tower	$\sigma_u/U^* \pm$ StD	$\sigma_v/U^* \pm$ StD	$\sigma_w/U^* \pm$ StD
Observations at z=5 m			
Katrina T0	4.83 ± 1.16	4.39 ± 1.30	1.60 ± 0.53
Katrina T1 (a)	2.15 ± 0.49	1.71 ± 0.52	1.49 ± 0.41
Katrina T1 (b)	2.99 ± 0.41	1.99 ± 0.35	1.14 ± 0.20
Katrina T2 (a)	3.27 ± 0.53	2.65 ± 0.41	1.16 ± 0.17
Katrina T2 (b)	3.55 ± 0.22	2.58 ± 0.27	1.22 ± 0.15
Rita T0 (a)	3.72 ± 1.11	2.87 ± 0.80	1.01 ± 0.21
Rita T0 (b)	2.63 ± 0.48	2.05 ± 0.43	0.95 ± 0.07
Rita T3 (a)	3.17 ± 0.32	2.35 ± 0.26	1.51 ± 0.14
Rita T3 (b)	3.22 ± 0.74	1.94 ± 0.37	1.63 ± 0.51
Rita T5 (a)	2.84 ± 0.34	2.35 ± 0.42	0.97 ± 0.09
Rita T5 (b)	5.92 ± 1.46	4.02 ± 1.08	1.90 ± 0.54
Wilma T0 (a)	3.29 ± 0.81	2.43 ± 0.72	1.24 ± 0.29
Wilma T0 (b)	2.60 ± 0.24	1.82 ± 0.22	1.09 ± 0.08
Wilma T1 (a)	4.31 ± 1.55	2.34 ± 0.66	1.36 ± 0.42
Wilma T1 (b)	2.51 ± 0.50	1.52 ± 0.43	1.07 ± 0.14
Wilma T2 (a)	2.65 ± 0.62	1.87 ± 0.58	1.20 ± 0.10
Wilma T2 (b)	3.11 ± 0.91	2.25 ± 0.62	1.83 ± 0.60
Observations at z=10 m			
Katrina T0	4.69 ± 1.05	4.02 ± 1.02	1.97 ± 0.44
Katrina T1 (a)	3.00 ± 0.48	2.53 ± 0.80	1.24 ± 0.13
Katrina T1 (b)	2.41 ± 0.27	1.85 ± 0.20	1.01 ± 0.07
Katrina T2 (a)	2.85 ± 0.34	2.12 ± 0.39	1.36 ± 0.14
Katrina T2 (b)	4.32 ± 1.81	3.34 ± 1.69	1.79 ± 0.68
Rita T0 (a)	3.85 ± 0.73	2.96 ± 0.73	1.30 ± 0.26
Rita T0 (b)	3.88 ± 1.67	3.09 ± 1.28	1.50 ± 0.59
Rita T3 (a)	2.32 ± 0.28	1.52 ± 0.20	0.96 ± 0.06
Rita T3 (b)	2.27 ± 0.18	1.54 ± 0.11	1.06 ± 0.08
Rita T5 (a)	2.56 ± 0.40	2.24 ± 0.40	1.13 ± 0.13
Rita T5 (b)	4.19 ± 0.66	2.97 ± 0.52	1.63 ± 0.24
Wilma T0 (a)	2.13 ± 0.31	1.49 ± 0.24	0.97 ± 0.10
Wilma T0 (b)	2.84 ± 0.70	2.36 ± 0.45	1.40 ± 0.21
Wilma T1 (a)	2.40 ± 0.18	1.49 ± 0.18	0.86 ± 0.10
Wilma T1 (b)	3.82 ± 1.63	2.82 ± 1.38	1.50 ± 0.59
Wilma T2 (a)	2.85 ± 1.02	2.18 ± 0.95	1.21 ± 0.25
Wilma T2 (b)	2.17 ± 0.34	1.61 ± 0.22	1.00 ± 0.11

Table 7
Aerodynamic roughness lengths.

Hurricane and tower	Height (m)	$(z_0)_1$ (cm)	$(z_0)_2$ (cm)	Mean wind direction (deg)	$(z_0)_3$ (cm)	Mean wind direction (deg)	$(z_0)_4$ (cm)	Mean wind direction (deg)
Katrina T0	5	0.2	0.5	63	0.2 ± 0.1	60	–	–
	5	–	–	–	0.3 ± 0.2	33	–	–
	10	0.5	0.7	67	1.9 ± 1.0	62	–	–
	10	–	–	–	1.8 ± 0.9	37	–	–
Katrina T1	5	3.2	3.9	33	7.1 ± 1.7	36	4.9 ± 2.7	37
	5	3.3	2.9	244	2.1 ± 0.6	237	9.3 ± 3.5	242
	10	0.9	0.9	32	1.2 ± 0.3	28	–	–
	10	3.1	3.6	248	1.2 ± 0.6	248	3.3 ± 1.5	246
Katrina T2	5	0.4	0.6	24	0.3 ± 0.1	25	0.4 ± 0.3	28
	5	0.2	0.2	273	0.1 ± 0.1	301	–	–
	10	1.1	1.1	23	0.6 ± 0.3	23	1.6 ± 1.0	24
	10	0.01	–	272	0.04 ± 0.04	300	–	–
Rita T0	5	0.1	0.3	6	0.2 ± 0.2	3	–	–
	5	0.7	–	230	0.4 ± 0.2	227	–	–
	10	0.1	0.2	7	0.1 ± 0.0	4	–	–
	10	0.05	–	231	0.2 ± 0.1	229	–	–
Rita T3	5	9.9	9.3	358	11.7 ± 2.0	359	12.7 ± 3.9	359
	5	1.2	1.6	224	0.8 ± 0.3	221	2.0 ± 0.6	222
	10	40.4	40.6	3	35.2 ± 12.7	3	56.3 ± 13.4	5
	10	7.4	8.5	226	5.8 ± 1.3	222	5.5 ± 1.6	222
Rita T5	5	5.0	4.5	16	1.0 ± 0.4	12	6.5 ± 2.8	15
	5	–	–	211	0.01 ± 0.01	210	–	–
	10	14.2	13.9	16	9.1 ± 2.0	9	21.2 ± 8.1	13
	10	0.01	–	210	0.2 ± 0.1	210	–	–
Wilma T0	5	1.4	2.3	117	2.0 ± 0.9	117	–	–
	5	6.1	5.8	301	4.8 ± 1.4	301	6.1 ± 0.8	298
	10	13.3	14.5	117	6.5 ± 2.6	117	17.0 ± 4.1	117

Table 7 (*continued*)

Hurricane and tower	Height (m)	$(z_0)_1$ (cm)	$(z_0)_2$ (cm)	Mean wind direction (deg)	$(z_0)_3$ (cm)	Mean wind direction (deg)	$(z_0)_4$ (cm)	Mean wind direction (deg)
	10	4.1	0.2	299	14.6 ± 4.3	300	11.4 ± 2.5	117
Wilma T1	5	0.3	0.4	126	1.7 ± 1.4	126	2.9 ± 2.5	121
	5	1.4	2.3	277	0.4 ± 0.2	288	0.6 ± 0.3	288
	10	4.7	4.4	132	0.7 ± 0.3	129	5.7 ± 2.2	131
	10	0.04	0.07	284	0.4 ± 0.3	289	1.3 ± 0.7	289
Wilma T2	5	–	–	–	7.5 ± 1.6	132	10.8 ± 4.5	130
	5	5.2	4.6	136	2.8 ± 1.2	137	–	–
	5	1.9	3.3	287	8.2 ± 2.1	289	–	–
	10	4.2	4.0	133	16.8 ± 4.2	127	19.6 ± 6.6	128
	10	17.2	22.4	285	10.9 ± 5.2	287	20.1 ± 13.9	284

Note 1: '–' denotes insufficient data to perform calculations.
Note 2: $(z_0)_1$ and $(z_0)_2$ were calculated for each partition, while $(z_0)_3$ and $(z_0)_4$ were calculated from subsets of each partition.

Table 8
Turbulence integral scales with standard deviations (m).

Hurricane and tower	$L_x^u \pm$ StD (m)	$L_x^v \pm$ StD (m)	$L_x^w \pm$ StD (m)
Observations at z=5 m			
Katrina T0	127.8 ± 43.4	102.1 ± 44.8	18.1 ± 5.7
Katrina T1 (a)	225.6 ± 109.5	155.1 ± 190.0	49.7 ± 28.5
Katrina T1 (b)	83.2 ± 34.9	84.4 ± 32.2	18.2 ± 6.3
Katrina T2 (a)	146.9 ± 91.3	98.6 ± 95.2	18.1 ± 8.9
Katrina T2 (b)	98.3 ± 27.4	87.3 ± 46.2	12.2 ± 4.8
Rita T0 (a)	135.4 ± 47.3	115.1 ± 77.2	20.3 ± 6.2
Rita T0 (b)	89.3 ± 29.7	66.4 ± 34.3	14.1 ± 2.8
Rita T3 (a)	47.2 ± 21.1	34.4 ± 20.5	5.7 ± 1.4
Rita T3 (b)	80.4 ± 28.6	29.0 ± 11.6	13.6 ± 3.6
Rita T5 (a)	104.5 ± 51.1	66.1 ± 55.3	15.9 ± 3.2
Rita T5 (b)	136.5 ± 51.4	92.2 ± 64.6	18.1 ± 4.8
Wilma T0 (a)	95.8 ± 38.0	57.5 ± 27.8	16.1 ± 15.8
Wilma T0 (b)	101.0 ± 33.8	55.4 ± 19.9	9.5 ± 1.7
Wilma T1 (a)	97.4 ± 62.8	66.6 ± 32.9	26.7 ± 51.8
Wilma T1 (b)	136.3 ± 90.9	158.3 ± 173.6	24.1 ± 33.2
Wilma T2 (a)	88.6 ± 37.7	70.7 ± 37.1	10.9 ± 2.8
Wilma T2 (b)	146.4 ± 53.8	59.2 ± 40.4	18.5 ± 5.9
Observations at z=10 m			
Katrina T0	133.2 ± 38.9	110.7 ± 54.0	18.9 ± 5.6
Katrina T1 (a)	267.4 ± 165.7	243.5 ± 264.2	22.0 ± 8.8
Katrina T1 (b)	135.1 ± 51.2	68.6 ± 19.9	20.3 ± 4.2
Katrina T2 (a)	170.8 ± 110.5	121.3 ± 108.3	19.9 ± 4.4
Katrina T2 (b)	126.2 ± 43.0	104.5 ± 49.8	22.0 ± 11.8
Rita T0 (a)	147.2 ± 50.4	126.4 ± 84.9	20.1 ± 5.3
Rita T0 (b)	101.0 ± 35.6	64.8 ± 39.2	15.1 ± 2.9
Rita T3 (a)	74.4 ± 31.9	55.1 ± 49.1	11.2 ± 3.3
Rita T3 (b)	112.8 ± 41.9	49.4 ± 21.5	16.8 ± 2.8
Rita T5 (a)	107.7 ± 49.7	65.5 ± 52.1	18.8 ± 4.2
Rita T5 (b)	150.4 ± 58.3	84.7 ± 59.7	19.1 ± 5.1
Wilma T0 (a)	128.5 ± 49.7	62.8 ± 26.4	23.7 ± 22.5
Wilma T0 (b)	152.9 ± 60.4	66.0 ± 39.7	25.5 ± 9.5
Wilma T1 (a)	160.6 ± 78.4	86.2 ± 41.9	24.1 ± 11.5
Wilma T1 (b)	189.1 ± 142.2	106.3 ± 63.0	13.1 ± 3.5
Wilma T2 (a)	120.4 ± 54.4	59.5 ± 30.5	16.5 ± 4.0
Wilma T2 (b)	173.5 ± 64.4	85.3 ± 49.9	25.6 ± 8.8

and (2)—expressions derived from the logarithmic velocity law, where the *avg* subscript refers to the average values and the *ind* subscript refers to the respective individual values.

$$z_0 = e^{\ln(z) - 0.4(U/U^*)} \tag{1}$$

$$z_0 = e^{\ln(z) - 0.4(((\sigma_w/U^*)_{avg})/((\sigma_w/U)_{ind}))} \tag{2}$$

The approaches taken to derive the roughness lengths are as follows:

1. $(z_0)_1$ is derived by inserting the average value of U/U^* for each partition into Eq. (1).
2. $(z_0)_2$ is derived by performing a linear regression analysis on U as a function of U^* with least squares criterion (assuming the y-intercept ≈ 0) and evaluating the slope of the plot of U versus U^* for each partition to insert it into Eq. (1).
3. $(z_0)_3$ is derived from Eq. (2) using the average value of σ_w/U^* for each data set and the individual values of σ_w/U in order to obtain a set of roughness lengths that are subsequently averaged. This operation is conducted for ranges in the data set where the observations of σ_w/U are reasonably uniform and where the change in wind direction is within an acceptable range.
4. $(z_0)_4$ is derived from Eq. (1) using individual values of the parameter U/U^* to obtain a set of roughness lengths that can be

subsequently averaged for ranges where U/U^{*} is reasonably uniform and where the change in wind direction is within a tolerable range.

In most cases, the spread in the z_0 values for a single height/tower combination is confined to one decade. Ideally, the 5 m and the 10 m roughness lengths should be the same or at least very similar. This similarity of the 5 and 10 m roughness length exists in some approaches for Katrina T1, Katrina T2, Rita T0, and Wilma T1 (Table 7). However, for the remaining towers, the 10 m roughness length is larger than that obtained from data at 5 m. This may be attributed to the 5 m measurement being more sensitive to the immediate upwind fetch, which is usually flat, open terrain, than the 10 m observation. The 10 m measurement is more sensitive to the larger roughness obstacles (such as large vegetation or buildings) further upstream from the observation site.

9. Turbulence integral length scales

The three turbulence integral length scales, L_x^u, L_x^v, and L_x^w, were determined for each 15 min sample record, their average values

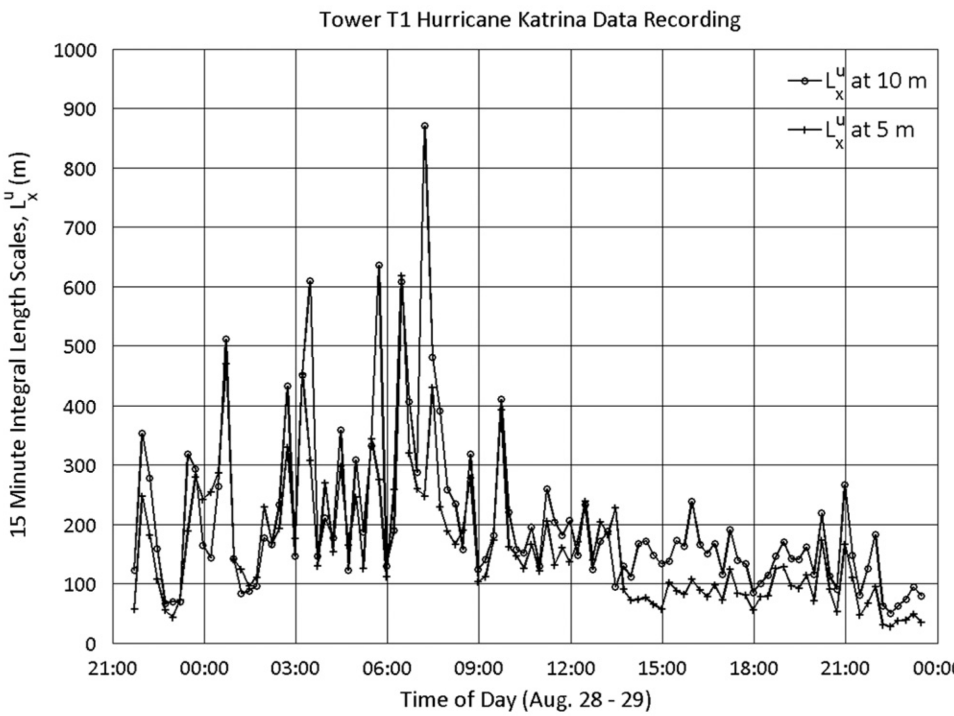

Fig. 8. Distribution of the L_x^u integral scale for hurricane Katrina, tower T1 at $z=5$ and 10 m (passage of the eye between 11:00 and 12:00 UTC).

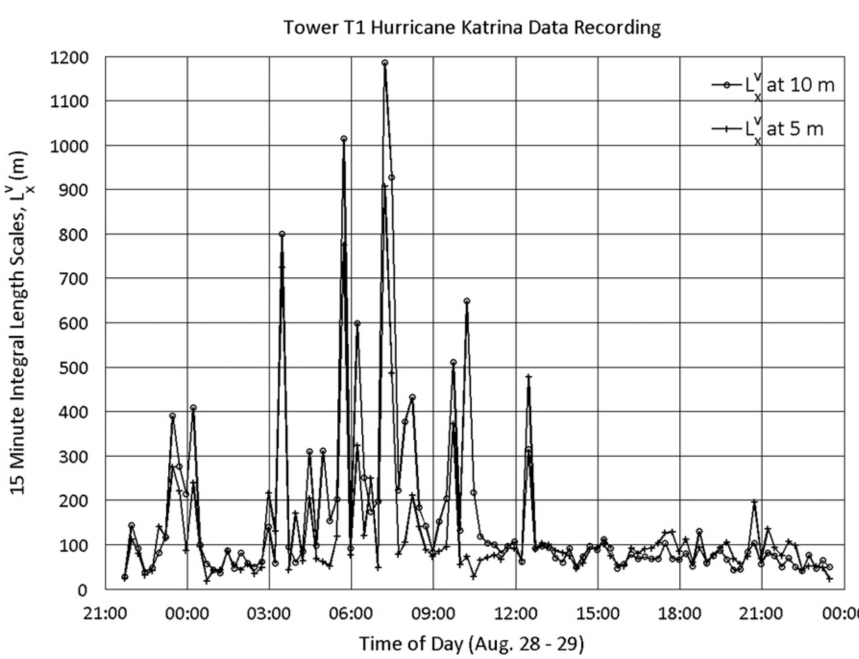

Fig. 9. Distribution of the L_x^v integral scale for hurricane Katrina, tower T1 at $z=5$ and 10 m (passage of the eye between 11:00 and 12:00 UTC).

are shown in Table 8 for each partition. Several different approaches have been employed in the literature to determine the length scale. For this analysis, sequential segments were linearly detrended and their along-wind velocity components were calculated. The scaled covariance (zero-mean and unit variance autocorrelation) function was then computed through Wiener–Khinchine relations, specifically through an inverse Fourier transform of the autospectrum estimate. Finally, the scaled covariance function was integrated numerically from $\tau=0$ s to the first crossing of the time lag, τ-axis, and multiplied by the segment's mean wind speed to estimate the length scale.

The observed values generally compare favorably with observations made by Counihan (1975), who estimated $L_x^u=196$ m for $z_0=0.01$ m and $L_x^u=139$ m for $z_0=0.03$ m. However, the peak integral length scales from each tower frequently exhibited large values (as large as 1200 m) for both horizontal scales (Figs. 8 and 9 for Katrina T1). The maximum values for the vertical scale, L_x^w, were in the 50 m range. The correlation between each of the horizontal scales at the 5 m and 10 m levels is quite high, most of its correlation coefficients exceed 0.9 (Table 9).

The correlation coefficients of the vertical scales at the two levels (ρ values below 0.5) are much lower than those of the horizontal scales. The results also show a low correlation between the L_x^u integral scale and the 3 s gust velocity (correlation coefficients well below 0.5 are shown in Table 10); as a result, large values of the integral scales cannot be associated with high values of the short duration peak velocities. Thus, it would not be expected that these large eddies are responsible for isolated swaths of damage to buildings and trees observed during damage assessments (e.g., Wakimoto and Black, 1994).

10. 3-s gust velocities

In addition to the 15 min mean velocity, the database also includes the maximum 3 s gust velocity for each 15 min sample record. The latter is the basic wind speed used in the *ASCE 7-10 Minimum Design Loads for Buildings and other Structures* (ASCE 7-10, 2010) at 10 m above the ground for a category C roughness exposure (Zhou and Kareem, 2002). The 3 s gust factor at a height of z meters above the ground, $G(3\text{ s}, z)$, and the normalized gust or the peak factor, $g(3\text{ s}, z)$, are defined in Eqs. (3) and (4), respectively.

$$G(3\,s,\,z)=\frac{U(3\,s,\,z)}{U(z)} \tag{3}$$

$$g(3\,s,\,z)=\frac{U(3\,s,\,z)-U(z)}{\sigma_u}=\frac{U(3\,s,\,z)}{\sigma_u}-TI_u \tag{4}$$

The 3 s gust speed, $U(3\text{ s}, z)$ from Eq. (4), can be substituted into Eq. (3) and one can obtain an expression for the 3 s gust factor,

Table 9
Correlation coefficients between L_x^u, L_x^v and L_x^w at 5 and 10 m.

Hurricane and tower	L_x^u	L_x^v	L_x^w
Katrina T0	0.944	0.950	0.406
Katrina T1	0.790	0.884	0.347
Katrina T2	0.927	0.957	0.387
Rita T0	0.917	0.956	0.487
Rita T3	0.827	0.804	0.694
Rita T5	0.967	0.984	0.498
Wilma T0	0.792	0.989	0.242
Wilma T1	0.899	0.886	−0.096
Wilma T2	0.900	0.921	0.414

Table 11
Average 3-s gust and peak factors.

Hurricane and tower	$GF(3\text{ s}, z)$	$g(3\text{ s}, z)$
Observations at z=5 m		
Katrina T0	1.841	3.246
Katrina T1 (a)	1.617	3.579
Katrina T1 (b)	1.744	3.037
Katrina T2 (a)	1.581	3.168
Katrina T2 (b)	1.523	2.947
Rita T0 (a)	1.569	3.190
Rita T0 (b)	1.489	3.058
Rita T3 (a)	2.028	3.152
Rita T3 (b)	1.664	3.114
Rita T5 (a)	1.819	3.279
Rita T5 (b)	1.513	3.012
Wilma T0 (a)	1.732	3.217
Wilma T0 (b)	1.744	3.126
Wilma T1 (a)	1.685	2.880
Wilma T1 (b)	1.492	2.874
Wilma T2 (a)	1.751	3.190
Wilma T2 (b)	1.735	3.330
Observations at z=10 m		
Katrina T0	1.798	3.180
Katrina T1 (a)	1.561	3.267
Katrina T1 (b)	1.530	3.158
Katrina T2 (a)	1.542	3.213
Katrina T2 (b)	1.504	3.149
Rita T0 (a)	1.543	3.198
Rita T0 (b)	1.469	3.032
Rita T3 (a)	1.812	2.795
Rita T3 (b)	1.572	3.068
Rita T5 (a)	1.795	3.253
Rita T5 (b)	1.503	3.016
Wilma T0 (a)	1.620	3.089
Wilma T0 (b)	1.626	3.004
Wilma T1 (a)	1.551	3.029
Wilma T1 (b)	1.463	2.936
Wilma T2 (a)	1.662	3.079
Wilma T2 (b)	1.664	3.102

Table 10
Comparison of L_x^u and $U(3\text{ s})$ at 10 m.

Hurricane and tower	Mean L_x^u (m)	Mean $U(3\text{ s})$ (m/s)	Standard deviation L_x^u (m)	Standard deviation $U(3\text{ s})$ (m/s)	Correlation coefficient
Katrina T0	95.5	13.94	48.3	8.81	0.550
Katrina T1	204.0	24.50	136.7	8.66	0.026
Katrina T2	156.1	30.53	87.5	6.37	0.128
Rita T0	140.7	25.66	56.4	7.9	0.292
Rita T3	95.7	24.74	41.0	6.16	−0.015
Rita T5	129.5	23.17	67.8	6.30	0.347
Wilma T0	136.6	19.94	53.6	8.54	0.269
Wilma T1	176.4	27.23	117.9	9.79	−0.038
Wilma T2	138.8	22.90	65.0	9.20	0.501

$G(3\text{ s}, z)$, as a function of the turbulence intensity (Eq. (5)).

$$G(3s, z) = 1 + \frac{g(3s, z)}{\frac{U(z)}{\sigma_u}} = 1 + g(3s, z)TI_u \quad (5)$$

Substituting the log law for neutral atmospheric conditions and accepting that σ_u/U^* and von Karman's constant are 2.5 and 0.4, respectively, Eq. (5) for the gust factor, $G(3\text{ s},z)$, can be rewritten as function of roughness length (Eq. (6)).

$$G(3s, z) = 1 + \frac{g(3s, z)}{\ln\left(\frac{z}{z_0}\right)} \quad (6)$$

It is evident from Eqs. (4)–(6) that gust and peak factors should vary with the roughness length, z_0, and/or the turbulence intensity, TI_u.

Average gust and peak factors for each partition are presented in Table 11. The gust factors are calculated using Eq. (3), where $U(3\text{ s},z)$ is the observed maximum 3 s gust for each 15 min record and $U(z)$, the corresponding hourly mean wind, is obtained by dividing the 15 min mean by 1.05, in accordance with the open-terrain gust factor distribution from Durst (1960). Peak factors were derived by solving Eq. (5) and using the observed turbulence intensity from the corresponding records. This approach will yield a conservative (higher) gust factor estimate since the use of a gust factor curve implies that the 15 min average is the peak such average within the hourly record. The Krayer and Marshall (1992) 3-s gust factor, 1.65, is higher than the average gust factor calculated for the partitions in Group 1, 1.524. However, the latter compares well to the Durst (1960) value of 1.51 and to the ESDU gust factor, 1.53, obtained by Vickery and Skerjl (2005) after analyzing tropical cyclone data for relatively smooth terrain.

The availability of individual gust factors under strong winds is of crucial importance in numerical or physical wind engineering, as these practices deal with and assess wind loads on buildings and structures. As an effort to satisfy this necessity, gust factors were obtained for the 15 min segments with maximum wind speed at the 10 m level for each tower. These gust factors, when plotted against the corresponding turbulence intensity (Fig. 10), exhibit a near linear variation with σ_u/U.

Analysis of the results depicted in Fig. 10 shows that a turbulence intensity of 17.7% corresponds to the generally

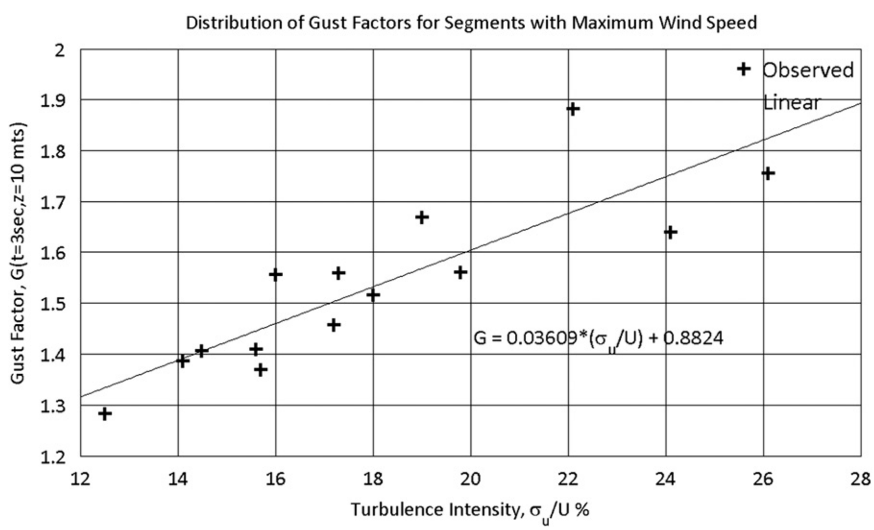

Fig. 10. Gust factor distribution with corresponding turbulence intensity for those segments with maximum wind speed (open exposure conditions correspond to TI_u=20% and $G(3, 10)$=1.52).

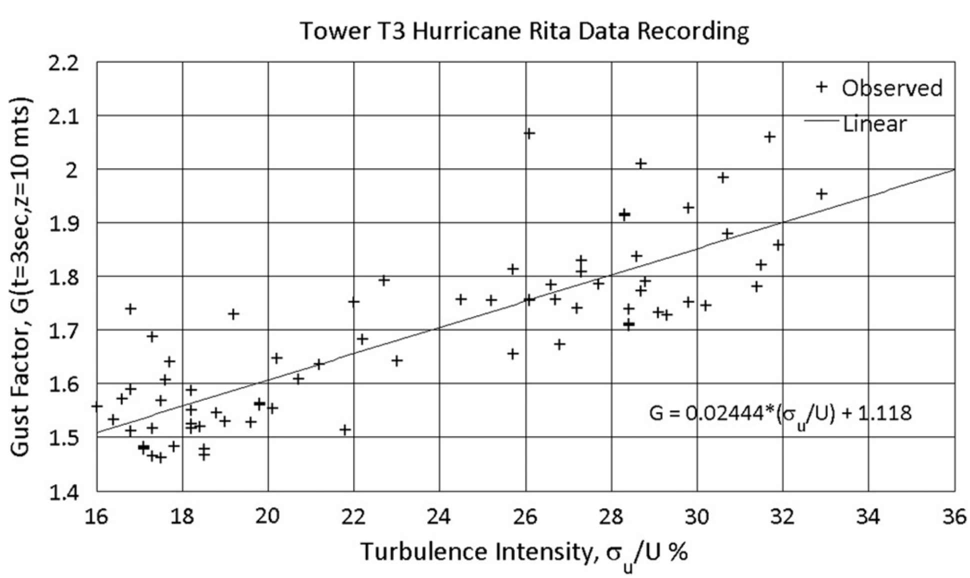

Fig. 11. Gust factor distribution with corresponding turbulence intensity for Rita T3 (open exposure conditions correspond to TI_u=20% and GF=1.52).

accepted gust factor value of 1.52. Neutral atmospheric flows with higher turbulence intensities are expected to have higher gust factor values; however, for flows having lower turbulence intensities lower gust factor values can be anticipated. Similar results for the entire data set from Rita T3 (Fig. 11) reveal a turbulence intensity of 16.5% for a 3 s gust factor of 1.52. The results from this study, which concur with the conclusion drawn by Vickery and Skerjl (2005) after analyzing land- and ocean-based weather systems, indicate that hurricane gust factors show a strong similarity to those of extra-tropical systems (e.g., winter storms).

Furthermore, it would be very instructive to obtain gust factors for the entire time range from 1 s to 1 h from the hurricane data. For this purpose one needs to select a group of four consecutive 15 min records for which the individual means are nearly equal. Location of a 1 h duration sample that is stationary with respect to mean flow and turbulence for data recorded in a fast moving hurricane is a challenging task. From the available data, the three most stationary 1-h records were selected to obtain gust factor distributions at near peak mean wind speeds. The gust factors were calculated according to Eq. (7), where $U(t)$ is the t-s gust speed obtained with a moving average and $U(T{=}3600\,\text{s})$ is the average wind speed for the 1 h record:

$$G(t, T = 3600s) = \frac{U(t)}{U(T = 3600s)} \tag{7}$$

The gust factor distributions are shown in Figs. 12–14 for Katrina T2 and Rita T3. As observed previously, the distributions

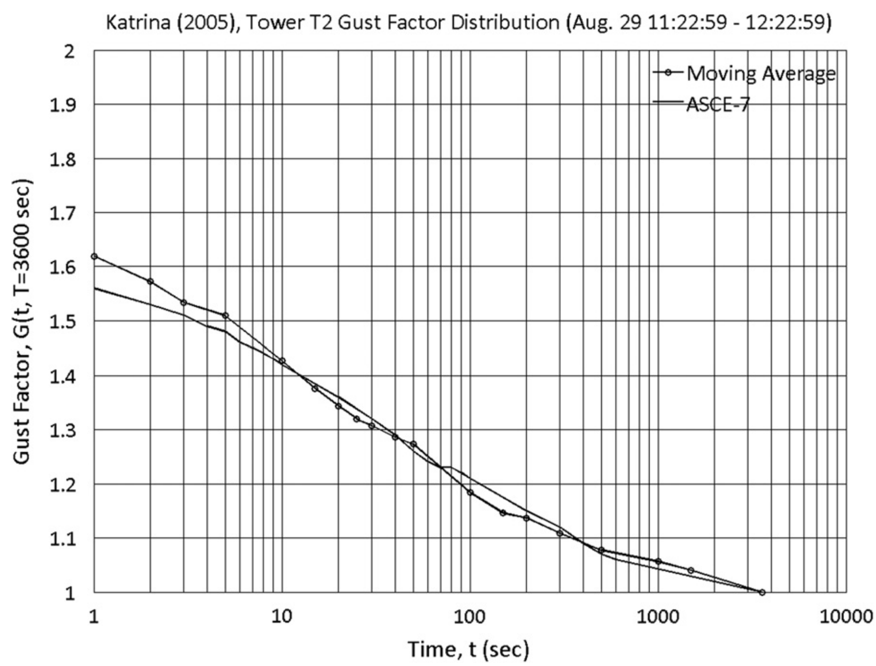

Fig. 12. Gust Factor distribution for Katrina T2 (files 36–39), U=27.37 m/s, σ_u/U=16.9% (UTC).

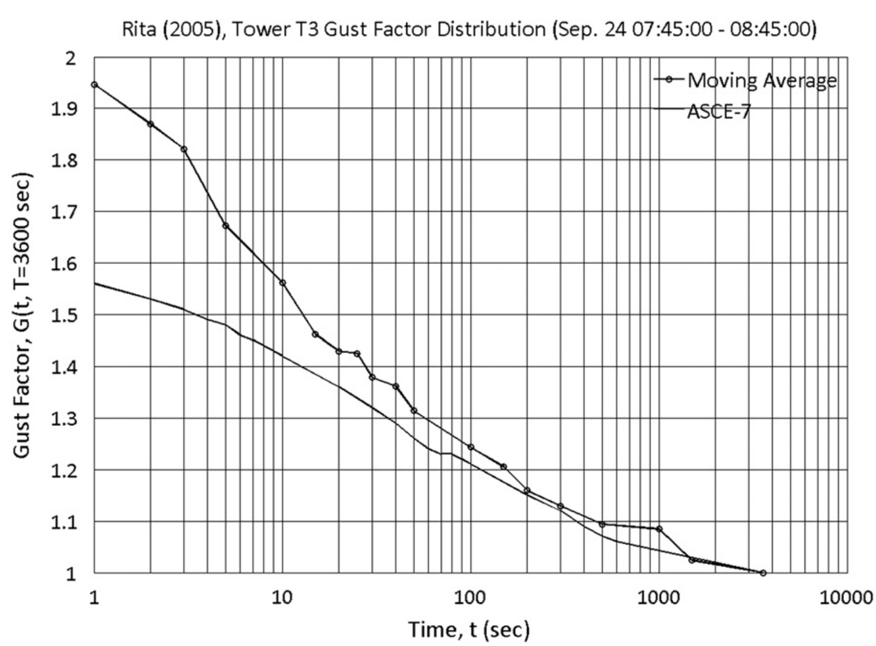

Fig. 13. Gust Factor distribution for Rita T3 (files 24–27), U=22.73 m/s, σ_u/U=26.8% (UTC).

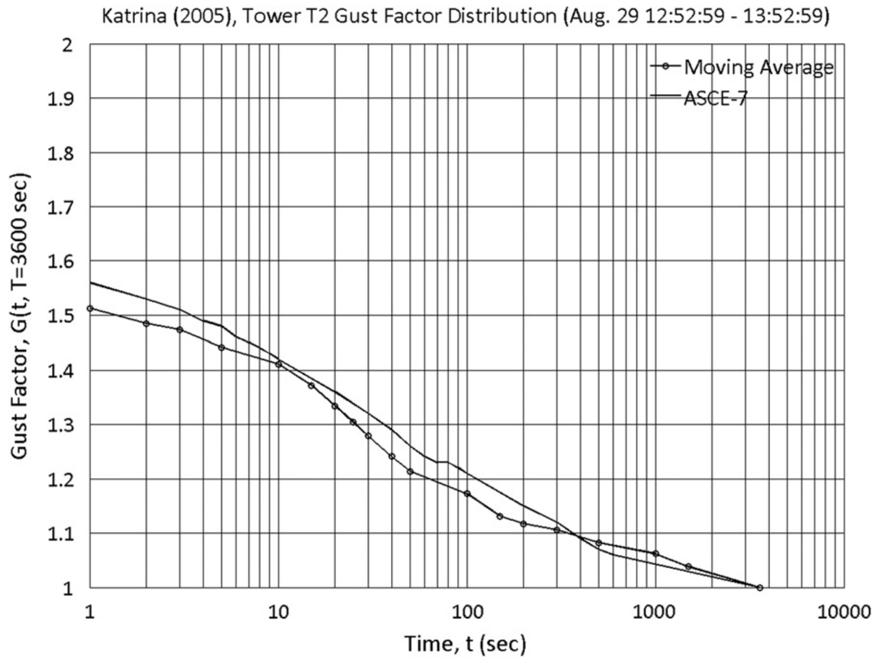

Fig. 14. Gust Factor distribution for Katrina T2 (files 42–45), U=26.49 m/s, σ_u/U=14.8% (UTC).

exhibit appreciable variation with turbulence intensity for short averaging times. The gust factor distribution for the data sample having a turbulence intensity of 16.9% matches the ASCE curve quite well (Fig. 12). The gust factor distribution from the sample with a turbulence intensity of 26.8% exceeds the ASCE curve considerably for low averaging times (Fig. 13). On the other hand, for the low turbulence-intensity sample (14.8%) the observed gust factors generally fall below the ASCE curve (Fig. 14).

11. Conclusions

Analyses of the ground winds observed during the passage of hurricanes reveal a considerable amount of similarity to extra-tropical strong winds. The mean winds show the passage of the hurricane eye with two velocity peaks and the associated near 180° change in wind direction. Nevertheless, some of the mean-wind records exhibit a single velocity peak together with the 180° wind direction change. The observed turbulence intensities and the turbulence derived aerodynamic roughness are associated with upwind terrain characteristics. Values of the observed *uw* covariance are mostly negative as one would expect in a standard boundary layer. The 3 s gust factor increases with increasing turbulence intensities and its value of 1.52 corresponds to an atmospheric flow with a turbulence intensity of approximately 17%.

Acknowledgements

The authors wish to thank the State of Florida Department of Community Affairs Residential Construction Mitigation Program and the NOAA Florida Hurricane Alliance for supporting hurricane deployment activities. Special recognition should be extended to Dr. Kurtis Gurley (University of Florida) and Dr. Timothy Reinhold (Institute for Business and Home Safety) for their pioneering efforts to establish the first in-situ wind engineering experiments during hurricane landfall. The authors also wish to thank Dr. Luis Aponte for his assistance in figure preparation. This work was supported in part by the National Science Foundation under Grant no. CMMI-0928563. Any opinions, findings, and conclusions or recommendations expressed in this material are those of the authors and do not necessarily reflect the views of the National Science Foundation.

References

ASCE 7-10, 2010. Minimum Design Loads for Buildings and Other Structures. American Society of Civil Engineers, Reston, VA.
Bradbury, W.M.S., Deaves, D.M., Hunt, J.C.R., Kershaw, R., Nakamura, K., Hardman, M.E., Hardman, P.W., 1994. The importance of convective gusts. Meteorological Applications 1, 365–378.
Counihan, J., 1975. Adiabatic atmospheric boundary layers—review and analysis of data from period 1880–1972. Atmospheric Environment 9 (10), 871–905.
Durst, C.S., 1960. Wind speeds over short periods of time. Meteorological Magazine 89, 181–1287.
Haan, F.L., Sarkar, P.P., Spencer-Berger, N.J., 2006. Development of an active gust generation mechanism on a wind tunnel for wind engineering and industrial aerodynamics applications. Wind and Structures 9 (5), 369–386.
Högström, U., 1990. Analysis of turbulence structure in the surface layer with a modified similarity formulation for near neutral conditions. Journal of Atmospheric Sciences 47, 55–78.
Izumi, Y., 1971, Kansas 1968 Field Program Data Report. Bedford, MA, Air Force Cambridge Research Papers, No. 379, 79pp.
Krayer, W., Marshall, R., 1992. Gust factors applied to hurricane winds. Bulletin of the American Meteorological Society 73 (5), 613–617.
Panofsky, H., Dutton, J., 1984. Atmospheric Turbulence, Models and Methods for Engineering Applications. Wiley International, NY, USA.
Salzano, C., Masters, F., Katsaros, J., 2010. Water penetration resistance of residential window installation options in hurricane prone areas. Building and Environment, 45 (6), 1373–1388.
Schroeder, J., Smith, D., 2003. Hurricane Bonnie wind flow characteristics as determined from WEMITE. Journal of Wind Engineering and Industrial Aerodynamics 91, 767–789.
Schroeder, J., Edwards, B., Giammanco, I., 2009. Observed tropical cyclone wind flow characteristics. Wind and Structures 12 (4), 347–379.
Vickery, P., Skerjl, P., 2005. Hurricane gust factors revisited. Journal of Structural Engineering 131 (5), 825–832.
Wakimoto, R.M., Black, P.G., 1994. Damage survey of Hurricane Andrew and its relationship to the eyewall. Bulletin of the American Meteorological Society 75 (2), 189–200.
Weber, R.O., 1999. Remarks on the definition and estimation of friction velocity. Boundary-Layer Meteorology 93, 197–209.

Wieringa, J., 1993. Representative roughness parameters for homogeneous terrain. Boundary-Layer Meteorology 63, 323–363.
Wurman, J., Winslow, J., 1998. Intense sub-kilometer-scale boundary layer rolls observed in Hurricane Fran. Science 280, 555–557.
Yu, B., Chowdhury, A., Masters, F., 2008. Hurricane power spectra, co-spectra, and integral length scales. Boundary-Layer Meteorology 129 (3), 411–430.
Zhou, Y., Kareem, A., 2002. Definition of wind profiles in ASCE 7. Journal of Structural Engineering 128 (8), 1082–1086.